Musical expertise is related to altered functional connectivity during audiovisual integration

Evangelos Paraskevopoulos[a,b], Anja Kraneburg[b,c], Sibylle Cornelia Herholz[d], Panagiotis D. Bamidis[a], and Christo Pantev[b,1]

[a]School of Medicine, Faculty of Health Sciences, Aristotle University of Thessaloniki, 54124 Thessaloniki, Greece; [b]Institute for Biomagnetism and Biosignalanalysis, University of Münster, 48149 Münster, Germany; [c]Research Group of Chronobiology, Leibniz Research Center for Working Enviroment and Human Factors, Dortmund, 44139 North Rhine-Westphalia, Germany; and [d]German Center for Neurodegenerative Diseases, 53175 Bonn, Germany

Edited by Josef P. Rauschecker, Georgetown University, Washington, DC, and accepted by the Editorial Board August 19, 2015 (received for review May 31, 2015)

The present study investigated the cortical large-scale functional network underpinning audiovisual integration via magnetoencephalographic recordings. The reorganization of this network related to long-term musical training was investigated by comparing musicians to nonmusicians. Connectivity was calculated on the basis of the estimated mutual information of the sources' activity, and the corresponding networks were statistically compared. Nonmusicians' results indicated that the cortical network associated with audiovisual integration supports visuospatial processing and attentional shifting, whereas a sparser network, related to spatial awareness supports the identification of audiovisual incongruences. In contrast, musicians' results showed enhanced connectivity in regions related to the identification of auditory pattern violations. Hence, nonmusicians rely on the processing of visual clues for the integration of audiovisual information, whereas musicians rely mostly on the corresponding auditory information. The large-scale cortical network underpinning multisensory integration is reorganized due to expertise in a cognitive domain that largely involves audiovisual integration, indicating long-term training-related neuroplasticity.

functional connectivity | MEG | multisensory integration | cortical plasticity | musical training

Multisensory integration is of such importance for our understanding of the surrounding world that its cortical correlates interact with most of the neocortical regions, including the ones traditionally considered as unisensory (1). The cortical areas that are usually referred to as multisensory include the superior temporal sulcus, the intraparietal sulcus, and the frontal cortex (2). Nevertheless, recent evidence suggests that multisensory perception engages more widespread areas than what the classic modular approaches have so far assumed (1). Moreover, audiovisual integration emerges from a dynamic interplay of distributed regions operating in large-scale networks (3).

The amount of shared information within these large-scale networks of distributed neuronal groups conceptualizes the notion of functional connectivity (4). Recent methodological advances allow the identification of networks that emerge from whole-brain analyses of neuroimaging data such as functional magnetic resonance imaging (fMRI) and magnetoencephalography (MEG) (5) and provide fertile ground for studying the functional connectivity patterns of higher cognitive processes. These kinds of networks are modeled as graphs composed of nodes, which represent the cortical areas contributing to the network, and by edges, which represent the connections between the nodes. Each network has specific attributes that quantify connectivity organization (6). These graphs depict the functional connectome of the respective cognitive processes. Recent evidence suggests that functional connectivity networks may be reorganized by factors mediating neuroplasticity such as learning and development (7), altering information processing pathways.

Music notation reading encapsulates auditory, visual, and motor information in a highly organized manner and therefore provides a useful model for studying multisensory phenomena (8). A recent study by Paraskevopoulos et al. (9) used MEG to reveal the cortical response related to identification of audiovisual incongruences. These incongruences occurred on the basis of an explicitly learned rule, binding otherwise unrelated unisensory stimuli. The rule was comparable to musical reading: "the higher the position of the circle, the higher the pitch of the tone." We recorded cortical responses to violations of this rule, to incongruences between expected auditory and visual input. This response was located in frontotemporal cortical areas. Plasticity effects related to long-term musical training were investigated in this cross-sectional study by comparison of musicians and nonmusicians, whereas effects of short-term music reading training were investigated in a follow-up longitudinal study that allowed causal inference of the neuroplastic effects (10).

A recent fMRI study by Lee and Noppeney (11) investigated how sensorimotor experience molds temporal binding of auditory and visual signals. The results of this study indicated that musicians exhibited increased audiovisual asynchrony responses and increased connectivity selectively for music, and not for speech, in a superior temporal sulcus–premotor–cerebellar circuitry that was defined and constrained by the corresponding fMRI activation results. Nevertheless, larger scale connectivity networks underpinning multisensory perception still remain undiscovered.

The goal of the present study was to investigate the functional connectivity of the cortical network underpinning audiovisual

Significance

Multisensory integration engages distributed cortical areas and is thought to emerge from their dynamic interplay. Nevertheless, large-scale cortical networks underpinning audiovisual perception have remained undiscovered. The present study uses magnetoencephalography and a methodological approach to perform whole-brain connectivity analysis and reveals, for the first time to our knowledge, the cortical network related to multisensory perception. The long-term training-related reorganization of this network was investigated by comparing musicians to nonmusicians. Results indicate that nonmusicians rely on processing visual clues for the integration of audiovisual information, whereas musicians use a denser cortical network that relies mostly on the corresponding auditory information. These data provide strong evidence that cortical connectivity is reorganized due to expertise in a relevant cognitive domain, indicating training-related neuroplasticity.

Author contributions: E.P., A.K., S.C.H., P.D.B., and C.P. designed research; E.P. performed research; E.P. contributed new reagents/analytic tools; E.P. analyzed data; and E.P., A.K., S.C.H., P.D.B., and C.P. wrote the paper.

The authors declare no conflict of interest.

This article is a PNAS Direct Submission. J.P.R. is a guest editor invited by the Editorial Board.

[1]To whom correspondence should be addressed. Email: pantev@uni-muenster.de.

This article contains supporting information online at www.pnas.org/lookup/suppl/doi:10.1073/pnas.1510662112/-/DCSupplemental.

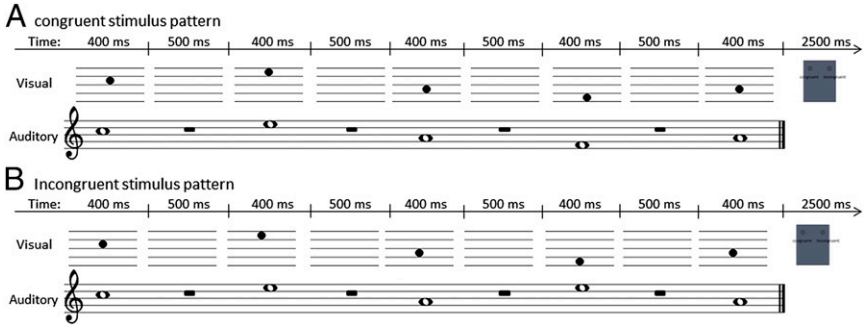

Fig. 1. Paradigm of an audiovisual congruent and incongruent trial. (*A*) A congruent trial. (*B*) An incongruent trial. The line "time" represents the duration of the presentation of the auditory and visual part of the stimulus. The last picture of each trial represents the intertrial stimulus in which subjects had to answer if the trial was congruent or incongruent.

integration, and particularly the identification of abstract audiovisual incongruences. Additionally, we aimed to address how this network is reorganized due to learning and whether expertise in a cognitive domain that largely involves audiovisual integration, such as music reading, may relate to changes in whole-brain functional connectivity. To this aim we used MEG to measure the cortical connectivity of a group of musicians and a group of musically naïve controls to congruent and incongruent audiovisual stimuli (Fig. 1). Source analysis was performed using a realistic head model to solve the forward problem and standardized low resolution electromagnetic tomography (sLORETA) (12) to solve the inverse one. The source time series were analyzed in terms of their underlying connectivity, by measuring their mutual information (MI) and applying a statistical model to extract the significant connections of the network. This approach allowed us to identify the corresponding whole-head, node-to-node network following a graph theoretical approach. Our hypothesis for this analysis was that a widespread network connecting cortical areas previously identified to be important for audiovisual integration would emerge. Regarding training effects, we anticipated that musicians would show greater connectivity between distributed cortical areas and that the network characteristics would indicate enhanced processing efficacy compared with the nonmusicians' network.

Results

Behavioral Responses. The behavioral responses of all subjects were used to calculate the discriminability index d prime. One-sample t tests for each group revealed that both groups scored significantly higher than chance level {musicians: 2.897 [t (12) = 78.414; $P < 0.001$]; nonmusicians: 1.68 [t (12) = 6.527; $P < 0.001$]}. Moreover, an independent-samples t test showed that musicians scored significantly higher than the controls [t (24) = 4.678; $P < 0.001$], indicating that musicians discriminated between the congruent and incongruent trials with greater accuracy than the nonmusicians. The d prime results are presented in Fig. S1.

Graph Analysis Results.

Cortical network underpinning audiovisual integration. The statistical analysis of the adjacency matrices of the group of musicians with the planned contrast of congruent > incongruent revealed a complex network of sources [$P < 0.001$; false discovery rate (FDR) corrected] compiled from 73 edges and 60 nodes, mainly right lateralized, connecting occipital (8 sources), parietal (10 sources), temporal (19 sources), and frontal (16 sources) areas (Fig. 2). The global efficiency of the network was found to be $E = 0.00063$, the density of the network was found to be $D = 0.00019$, whereas the node strength identified that the node with the greatest sum of strengths was located in the right precentral gyrus. The analysis of the adjacency matrices of the group of nonmusicians with the planned contrast of congruent > incongruent revealed a different network of sources ($P < 0.001$; FDR corrected) compiled from 62 edges and 62 nodes, connecting mainly occipital (7 sources), parietal (12 sources), temporal (12 sources), and frontal (22 sources) areas (Fig. 2). In contrast to the musicians' network, the nonmusicians' network was lateralized mainly toward the left hemisphere. The global efficiency of the network was found to be $E = 0.00041$, the density of the network was found to be $D = 0.00016$, whereas the node strength identified that the node with the greatest sum of strengths was located in the left middle frontal gyrus.

The between-groups comparison revealed that the congruent > incongruent network of the musicians differed significantly ($P < 0.001$; FDR corrected) from the one of nonmusicians, showing greater connectivity in a network compiled from 68 edges and 49 nodes, mainly connecting temporal (17 sources) and frontal (18 sources) areas as well as parietal (7 sources) and occipital (2 sources) ones (Fig. 2). The node with the greatest sum of strengths was located in the right precentral gyrus. The statistical map of this analysis, along with the corresponding node strengths, is presented in Fig. 2.

Cortical network underpinning audiovisual incongruency identification. The statistical analysis of the adjacency matrices of the group of musicians with the planned contrast of incongruent > congruent revealed a complex network of sources ($P < 0.05$; FDR corrected) compiled from 85 edges and 71 nodes, mainly right lateralized, connecting occipital (11 sources), parietal (20 sources), temporal (3 sources), and frontal (29 sources) areas (Fig. 3). The global efficiency of the network was found to be $E = 0.00049$, the density of the network was found to be $D = 0.00022$, whereas the node strength identified that the node with the greatest sum of strengths was located in the right postcentral gyrus. The analysis of the adjacency matrices of the group of nonmusicians with the planned contrast of incongruent > congruent revealed a sparser network of sources ($P < 0.05$; FDR corrected) compiled from 10 edges and 14 nodes, connecting mainly parietal (10 sources) and frontal (12 sources) areas but also occipital (2 sources), and temporal (4 sources) ones (Fig. 3). The global efficiency of the network was found to be $E = 0.00026$, the density of the network was found to be $D = 0.00003$, whereas the node with the greatest sum of strengths was located in the left postcentral gyrus.

The between-groups comparison revealed that the incongruent > congruent network of the musicians differed significantly ($P < 0.05$; FDR corrected) from the one of nonmusicians, showing greater connectivity in a network compiled from 94 edges and 112 nodes, mainly connecting frontal (36 sources), temporal (25 sources), parietal (14 sources), and occipital (16 sources) areas (Fig. 3). The node with the greater sum of strengths was located in the left inferior frontal gyrus. The statistical map of this analysis, along with the corresponding node strengths are presented in Fig. 3 and the network organization parameters are presented in Table 1.

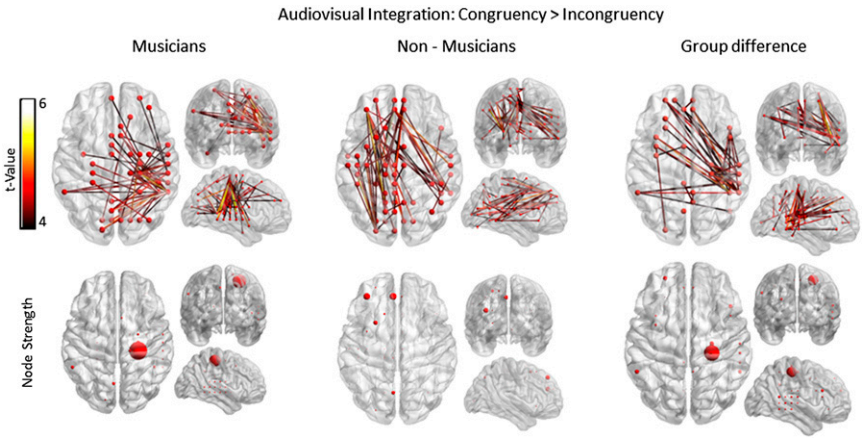

Fig. 2. Cortical network underpinning audiovisual integration. (*Upper*) Statistical parametric maps of the significant networks for the congruent > incongruent comparison. Networks presented are significant at $P < 0.001$, FDR corrected. The color scale indicates t values. (*Lower*) Node strength of the significant networks for each comparison. Strength is represented by node size.

Discussion

The present study investigated the cortical large-scale functional network supporting audiovisual integration. The reorganization of this network related to long-term musical training was investigated by comparing musicians to nonmusicians. Magnetoencephalographic recordings were used to measure cortical responses. Large-scale connectivity of the cortical activity was calculated via a statistical comparison of the estimated MI in the sources' activity. The results indicated a dense cortical network underpinning multisensory integration, whereas a relatively sparser network supports the identification of abstract audiovisual incongruences. Musicians show greater connectivity than nonmusicians between distributed cortical areas, including a greater contribution of the right temporal cortex for multisensory integration and the left inferior frontal cortex for identifying abstract audiovisual incongruences. Moreover, the network organization of musicians indicates enhanced processing efficiency.

The behavioral results are in line with previously reported ones (9), indicating that musicians' prior experience in musical reading is associated with a behavioral benefit. Previous psychophysical studies have reported similar results among nonmusicians, indicating that the identification of cross-modal correspondences between pitch height and the height of a visual stimulus may be innate (13). In contrast, a recent study by our group investigating the audiotactile integration (14) indicated that similar rules binding auditory and tactile stimuli were not intrinsically incorporated by the nonmusicians, but that musical expertise was essential for reaching correct identification of audiotactile incongruences.

The statistical comparison of the individual cortical connectivity matrices indicated that when nonmusicians were confronted with congruent audiovisual trials they activated a large-scale functional network that followed a mainly dorsal pathway. Although this network consists of distributed sources, there is a prominent contribution of connections between occipitoparietal and frontal regions. Sources located in superior and middle temporal gyrus contribute to a lesser extent, having direct connections with the middle occipital gyrus and the superior frontal one. The dorsal visual (15) pathway is thought to be responsible for the processing of spatial information, receiving much of its input from magnocellular cells (16). The structural substrates of the dorsal auditory pathway (17, 18) are mainly the superior longitudinal fasciculus and the arcuate fasciculus that connects the superior temporal gyrus with the dorsal prefrontal cortex (19, 20). This pathway has been associated with attentional shifting (21) and behavioral choices for visual stimuli in both target-present and target-absent conditions, predicting choice accuracy (22). The cortical organization of this large-scale network indicates that nonmusicians rely heavily on the processing of the corresponding visual cues for the integration of congruent audiovisual information.

In contrast, the large-scale network used by musicians for identifying congruent audiovisual information shows significantly greater connectivity between distributed cortical sources. Direct connections between occipital and frontal sources contribute to multisensory perception; nevertheless, the prominent role of right superior and middle temporal gyri indicates an important role of auditory information processing in this network. This result is in line with recent neurophysiological evidence, indicating that musicians show greater activation of the right middle and superior temporal gyri, which is correlated with increased sensitivity to acoustic features and enhanced selective attention to temporal features of speech (23). The comparison of the networks used by musicians and nonmusicians reveals significant differences in the connectivity of the temporal sources with precentral and frontal ones. This result seems to depict the audiovisual-motoric binding that musicians have highly trained to read musical scores and to play their instrument (24). This binding was recently shown also by an MEG study of our group (14), revealing how musical training molds the neural correlates of an integrative audiotactile response. Moreover, musicians show increased connectivity of the temporal sources with the prefrontal

Table 1. Global efficiency and density values of the significant networks of musicians and nonmusicians for each condition

Condition	Network organization parameter	Musicians	Nonmusicians
Congruent > incongruent	Global efficiency	0.00063	0.00041
	Density	0.00019	0.00016
Incongruent > congruent	Global efficiency	0.00049	0.00026
	Density	0.00022	0.00003

cortex, a result that is in line with diffusion tensor imaging (DTI) studies, indicating increased functional anisotropy of the right arcuate fasciculus in musicians (25). In these studies, the increase of functional anisotropy was attributed to increased myelination, caused by neural activity in fiber tracts during training. In addition, the network organization parameters indicate that the functional connectivity pattern that musicians use to process congruent audiovisual information shows greater efficiency and is denser than the corresponding network of the nonmusicians, reflecting enhanced multisensory processing.

The statistical analysis of the cortical connectivity of nonmusicians underpinning abstract audiovisual identification (Fig. 3) revealed a sparser network, as indicated also by its low density and efficiency. This network connects mainly parietal and frontal areas, receiving input also from occipital (cuneus) and temporal (transverse temporal gyrus) sources, indicating combined top-down and bottom-up processing. The main connections of inferior parietal and frontal sources closely correspond to the pathway subserving visual spatial awareness. Its structural substrate is linked to superior occipitofrontal fasciculus (26). This system seems to be dissociated from auditory spatial processing (27). Nevertheless, our results indicate significant functional connectivity with the transverse temporal gyrus, most likely supporting a bottom-up process underpinning a multisensory component (28). In addition, coactivation, and thus connectivity, in these areas has been correlated with working memory tasks (29). These cognitive functions serve an important role in identifying the abstract audiovisual incongruences presented in the paradigm of this study and may be interpreted, in resemblance to the multisensory integration network, as indications that nonmusicians recruit stronger contribution from the processing of visual information for identifying the incongruences.

The group of musicians employs a large-scale cortical network to identify abstract audiovisual incongruences. This network consists mainly of long-range occipitofrontal and parietofrontal connections, having edges also to the right middle and superior temporal gyrus. Its general structure indicates the use of superior longitudinal and arcuate fasciculus (30), resembling the network used by nonmusicians for the identification of congruent multisensory information, although being more strongly lateralized to the right hemisphere. The statistical analysis of the group differences for this condition indicates the significantly greater contribution of the left inferior frontal cortex in the network connectivity in musicians compared with nonmusicians. Specifically, this analysis indicates that musicians show enhanced connectivity in a large-scale network that employs both the dorsal and ventral pathway for the long-range connections and relies greatly on the contribution of the left inferior frontal cortex. The organization of this network indicates that musicians make greater use of the temporal sources (and auditory information accordingly). The present results closely relate to previous results reported by our group (9, 10). This analysis further revealed that musicians showed significantly greater activity than nonmusicians in superior frontal, superior temporal, and lingual gyrus when confronted with incongruences. More importantly, the significant role of inferior frontal cortex for response inhibition (31) and for the identification of auditory pattern violations (32, 33) has been repeatedly shown using several neuroimaging modalities (34) not only for linguistic (35) but also for musical stimuli (36). In addition, musicians show enhanced gray matter density (37) and enhanced connectivity of this region (38). Functional MRI evidence links this area to the processing of audiovisual speech (39) as well as the enhanced visuospatial processing of musicians (40) and thus, it may ideally serve the superior identification of abstract audiovisual incongruences that musicians show in this study. The network organization parameters reveal that the network of musicians has enhanced density and processing efficiency. It has to be noted here that functional connectivity as measured in the present study has been shown to closely relate to structural connectivity (41), nevertheless, functional connectivity analysis also provides different and complementary information (42).

Conclusion

The present study revealed for the first time to our knowledge the large-scale functional network underpinning audiovisual integration as well as the effect of musical expertise on reorganizing this network. A novel approach for graph theoretical analysis of MEG data revealed that nonmusicians rely heavily on the processing of corresponding visual clues for the integration of audiovisual information, whereas in contrast, musicians use more temporal sources along with the left inferior frontal gyrus. Hence, the results suggest that large-scale functional connectivity subserving multisensory integration is reorganized due to expertise in a cognitive domain that largely involves audiovisual integration, such as music reading, indicating that the corresponding cortical network forms a dynamic system that can be affected by long-term training.

Methods

Subjects. A new dataset was created for the present study from MEG measurements that have been presented in two previous publications (9, 10). In the new dataset, we included the same number of musicians and nonmusicians for

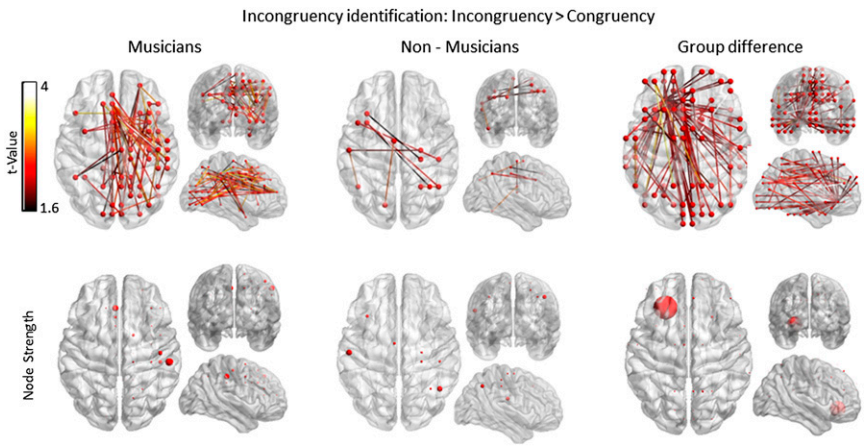

Fig. 3. Cortical network underpinning audiovisual incongruency identification. (*Upper*) Statistical parametric maps of the significant networks for the incongruent > congruent comparison. Networks presented are significant at $P < 0.05$, FDR corrected. The color scale indicates t values. (*Lower*) Node strength of the significant networks for each comparison. Strength is represented by node size.

whom MRI data were available. Hence, 26 individuals participated in the present study, 13 musicians and 13 nonmusicians. Musicians (mean age = 25.32; SD = 2.68; five males) were retrieved from the pool of students of the Music Conservatory of the University of Münster (mean musical training = 17.23; SD = 3.81). Nonmusicians (mean age = 26.46; SD = 2.66; six males) had not received any formal musical education apart from compulsory school lessons. All subjects were right handed according to the Edinburgh Handedness Inventory (43) and had normal hearing as evaluated by clinical audiometry. Subjects provided written informed consent before their participation in the study. The study protocol was approved by the ethics committee of the medical faculty of the University of Münster and the study was conducted according to the Declaration of Helsinki.

Stimuli. Audiovisual congruent and incongruent stimuli were prepared by combining melodies that consisted of five tones with five images representing the pitch height of each tone. Each image presented five white horizontal lines against a black background, similar to the staff lines in music notation. A blue disk (RGB color codes: red, 86; green, 126; and blue, 214) was then placed in the middle of the screen on the horizontal axis and in one of the four spaces between the lines. The five-tone melodies were constructed by the combination of four sinusoidal tones (F5, 698.46 Hz; A5, 880.46 Hz; C6, 1046.50 Hz; and E6, 1318.51 Hz) with duration of 400 ms including 10-ms rise and decay time (48,000 Hz, 16 bit). The interstimulus interval (stimulus offset to stimulus onset, ISI) between each tone was set to 500 ms and the total duration of each melody was 4 s. Eight different trials of five-tone melodies and five images were prepared for each condition (i.e., congruent and incongruent, respectively).

For the audiovisual "congruent" trials, the melodies were combined with the corresponding image according to the rule "the higher the pitch, the higher the position of the disk," thus following a similar rule of ordinal relationship that the Western music notation system uses. During the acoustic presentation of each tone, the corresponding disk was presented visually at the middle of the screen, at the exact same time, and for the same duration as the tone. During the ISI, a fixation cross was presented. The audiovisual "incongruent trials" were prepared along the same principles as the congruent ones, except that one of the tones of the melodies was paired with an image that did not correspond to the tone according to the above-mentioned rule. The incongruency was never in the first or last tone–number pair, but occurred at all of the other three positions with equal probabilities (Fig. 1).

Experimental Design.

MEG recordings. Evoked magnetic fields were recorded with a 275-channel whole-head system (OMEGA, CTF Systems) in a magnetically shielded room. Data were acquired continuously with a sampling rate of 600 Hz. Subjects were seated upright, and their head position was comfortably stabilized with pads inside the MEG dewar. The auditory stimulation was delivered via 60-cm-long silicon tubes at 60 dB SL above the individual hearing threshold that was determined with an accuracy of at least 5 dB at the beginning of each MEG session for each ear. Visual stimuli were projected with an Optoma EP783S DLP projector and a refresh rate of 60 Hz onto the back of a semitransparent screen positioned ∼90 cm in front of the subjects' nasion. The viewing angle ranged from −3.86° to 3.86° in the horizontal direction and from −1.15° to 1.15° in the vertical direction.

The congruent and incongruent trials were randomly interleaved in one run. The continuous recording was time locked to the presentation of the second, third, and fourth tones/images of the audiovisual congruent patterns and the presentation of the incongruent tone/image of the audiovisual incongruent patterns. This procedure resulted in an incongruent (deviant) to congruent (standard) ratio of 33.3%. Within 2.5 s after each trial, subjects had to answer via button pressings if the trial was congruent or incongruent (right hand). During this intertrial interval, an image was presented to the subjects reminding them which button represented each answer. Subjects were exposed to four measurement runs, lasting ∼14.5 min each, with short breaks in between. The total number of trials for each condition was 104.

MRI protocol. Before the experiment, T1-weighted MR images from each individual were obtained in a 3-Tesla scanner (Gyroscan Intera T30, Philips). These anatomical scans served for constructing the individualized finite element models (FEMs) that were then used in the source reconstruction. A total of 400 contiguous T1-weighted slices of 0.5-mm thickness in the sagittal plane (TR = 7.33.64 ms, TE = 3.31 ms) were collected by a Turbo Field Echo acquisition protocol. The field of view was set to 300 × 300 mm with an in-plane matrix of 512 × 512 setting defining the native voxel size at 0.5 × 0.58 × 0.58 mm^3. Using SPM8 (Statistical Parametric Mapping, www.fil.ion.ucl.ac.uk) the intensity bias of the images was then regularized to account for intensity differences within each tissue, and the images were resliced to isotropic voxels of 1.17 × 1.17 × 1.17 mm.

MEG Data Analysis.

Source activity estimation. The Brain Electrical Source Analysis software (BESA Research, version 6, Megis Software) was used for the preprocessing of the MEG data. Artifacts due to blinks or eye movements were corrected by applying an adaptive artifact correction (44). The recorded data were separated in epochs of 1 s, including a prestimulus interval of 200 ms. Epochs were baseline corrected using the interval from −100 to 0 ms. From each congruent trial only one randomly selected tone–number pair was included in the analysis, thus producing an equal number of congruent and incongruent epochs. Data were filtered offline with a high-pass forward filter of 1 Hz, a low-pass zero-phase filter of 30 Hz, and an additional notch filter at 50 Hz. Epochs containing signals larger than 2.5 picotesla in the MEG were considered as artifact contaminated and excluded from averaging. The congruent and incongruent trials of each run were separately averaged.

BESA MRI was used to construct individual FEM models. The individual positions of the MEG sensors were coregistered via anatomical landmarks (nasion, left and right preauricular points) to each subject's structural MRI. Transformation to anterior commissure - posterior commissure and Talairach space was performed by direct 3D-spline interpolation of the original MRI. A finite element model, based on the segmentation of four different head tissues [i.e., scalp, skull, cerebrospinal fluid (CSF), and brain], was computed for each participant on the basis of their individual structural MRI and used as a volume conductor model. The conductivity value for the skin compartment was set to 0.33 S/m, for the skull compartment to 0.0042 S/m, for the brain to 0.33 S/m, and for the CSF to 0.79 S/m as proposed in ref. 45. The use of realistic FEMs generated on the basis of the individual anatomy of each subject improves the source localization reliability of the MEG signals, especially when the compartment of CSF is included in the model (46).

Current density reconstructions (CDRs) were calculated on the neural responses of each subject separately for each run's congruent and incongruent averages using the sLORETA method (12) as provided by BESA. This method is an unweighted minimum norm that is standardized by the resolution matrix. Hence, it has the advantage of not needing an a priori definition of the number of activated sources. Each individual's CDRs were calculated for the complete response time window (i.e., 0–800 ms) of each condition, each run, and for each sample point. The CDRs were exported from BESA as four-dimensional (4D) nifti images and the images of each run were then averaged, resulting in one 4D image of 480 samples for each subject and each condition. The images were then processed with a mask that included only the gray matter and excluded the brainstem and cerebellum to limit the source space. This procedure resulted in a source space of 863 voxels.

Graph analysis. The CDR voxel time series were extracted in order for the connectivity matrices to be calculated, whereas a node of the network was appointed to each voxel of the masked 4D images (resulting in 863 nodes). The Matlab R2010a (MathWorks) toolbox HERMES (47) was used for calculating the 863 × 863 adjacency matrix from the voxel time series (i.e., the 4D images) of each subject and each condition was based on the algorithm of MI. MI quantifies the amount of information that is obtained for a random variable by observing another. The main advantage of MI is that, being based on nonlinear probability distributions, it detects higher order correlations. Therefore, its result is not dependent on any specific model of the data (47).

The toolbox Network Based Statistic (NBS) (48) was used to statistically identify significant connections in the graphs, using a general linear model approach that compares the connectivity values of each node and for each subject and condition. Specifically, a mixed model ANOVA with a between-subject factor group and a within-subject factor condition was designed to explore the main effect of condition within each group and the group × condition interaction via planned contrasts. The significance level was set to $P < 0.05$ (or $P < 0.001$ when noted accordingly) corrected for multiple comparisons via FDR correction. The visualization of the significant networks as weighted graphs was performed using BrainNet Viewer (49).

To investigate the functional connectivity parameters and the efficacy of the networks, the graph properties of global efficiency, network density, and node strength were calculated for the significant networks, as resulted from the NBS analysis. The global efficiency is the average inverse shortest path length in the network, reflecting the level of global integration in the network. In other words, global efficiency depicts the average number of nodes through which the information flows to reach a distant point of the network. The fewer nodes that intervene in the information flow, the greater the efficiency of the network. The node density is the fraction of present connections to possible connections, indicating how many of the available cortical areas actually contribute to the network, whereas the node strength sums the weights (i.e., *t* values in the present analysis) of links connected to the node, thus identifying the nodes that show greater connectivity differences. These properties were calculated using the Brain Connectivity Toolbox (50).

ACKNOWLEDGMENTS. This work was partly supported by the Deutsche Forschungsgemeinschaft (Grant PA392/12-2) and partly by an internal research fellowship from the Research Committee of the Aristotle University of Thessaloniki (Award 31663/2014).

1. Ghazanfar AA, Schroeder CE (2006) Is neocortex essentially multisensory? *Trends Cogn Sci* 10(6):278–285.
2. Schroeder CE, Foxe J (2005) Multisensory contributions to low-level, 'unisensory' processing. *Curr Opin Neurobiol* 15(4):454–458.
3. Zamora-López G, Zhou C, Kurths J (2010) Cortical hubs form a module for multisensory integration on top of the hierarchy of cortical networks. *Front Neuroinform* 4:1.
4. Greicius MD, Krasnow B, Reiss AL, Menon V (2003) Functional connectivity in the resting brain: A network analysis of the default mode hypothesis. *Proc Natl Acad Sci USA* 100(1):253–258.
5. Bullmore E, Sporns O (2009) Complex brain networks: Graph theoretical analysis of structural and functional systems. *Nat Rev Neurosci* 10(3):186–198.
6. Stam CJ, Reijneveld JC (2007) Graph theoretical analysis of complex networks in the brain. *Nonlinear Biomed Phys* 1(1):3.
7. Supekar K, Musen M, Menon V (2009) Development of large-scale functional brain networks in children. *PLoS Biol* 7(7):e1000157.
8. Herholz SC, Zatorre RJ (2012) Musical training as a framework for brain plasticity: Behavior, function, and structure. *Neuron* 76(3):486–502.
9. Paraskevopoulos E, Kuchenbuch A, Herholz SC, Pantev C (2012) Musical expertise induces audiovisual integration of abstract congruency rules. *J Neurosci* 32(50): 18196–18203.
10. Paraskevopoulos E, Kuchenbuch A, Herholz SC, Pantev C (2014) Multisensory integration during short-term music reading training enhances both uni- and multisensory cortical processing. *J Cogn Neurosci* 26(10):2224–2238.
11. Lee H, Noppeney U (2011) Long-term music training tunes how the brain temporally binds signals from multiple senses. *Proc Natl Acad Sci USA* 108(51):E1441–E1450.
12. Pascual-Marqui RD (2002) Standardized low-resolution brain electromagnetic tomography (sLORETA): Technical details. *Methods Find Exp Clin Pharmacol* 24(Suppl D):5–12.
13. Spence C, Deroy O (2013) How automatic are crossmodal correspondences? *Conscious Cogn* 22(1):245–260.
14. Kuchenbuch A, Paraskevopoulos E, Herholz SC, Pantev C (2014) Audio-tactile integration and the influence of musical training. *PLoS One* 9(1):e85743.
15. Ungerleider LG, Mishkin M (1982) Two cortical visual systems. *Analysis of Visual Behavior*, eds Ingle MA, Goodale MI, Masfield RJW (MIT Press, Cambridge, MA), pp 549–586.
16. Logothetis NK, Sheinberg DL (1996) Visual object recognition. *Annu Rev Neurosci* 19: 577–621.
17. Rauschecker JP, Tian B (2000) Mechanisms and streams for processing of "what" and "where" in auditory cortex. *Proc Natl Acad Sci USA* 97(22):11800–11806.
18. Rauschecker JP, Scott SK (2009) Maps and streams in the auditory cortex: Nonhuman primates illuminate human speech processing. *Nat Neurosci* 12(6):718–724.
19. Saur D, et al. (2008) Ventral and dorsal pathways for language. *Proc Natl Acad Sci USA* 105(46):18035–18040.
20. Glasser MF, Rilling JK (2008) DTI tractography of the human brain's language pathways. *Cereb Cortex* 18(11):2471–2482.
21. Pammer K, Hansen P, Holliday I, Cornelissen P (2006) Attentional shifting and the role of the dorsal pathway in visual word recognition. *Neuropsychologia* 44(14):2926–2936.
22. Donner TH, et al. (2007) Population activity in the human dorsal pathway predicts the accuracy of visual motion detection. *J Neurophysiol* 98(1):345–359.
23. Jantzen MG, Howe BM, Jantzen KJ (2014) Neurophysiological evidence that musical training influences the recruitment of right hemispheric homologues for speech perception. *Front Psychol* 5:171.
24. Schön D, Anton JLJL, Roth M, Besson M (2002) An fMRI study of music sight-reading. *Neuroreport* 13(17):2285–2289.
25. Wan CY, Schlaug G (2010) Music making as a tool for promoting brain plasticity across the life span. *Neuroscientist* 16(5):566–577.
26. Thiebaut de Schotten M, et al. (2005) Direct evidence for a parietal-frontal pathway subserving spatial awareness in humans. *Science* 309(5744):2226–2228.
27. Kong L, et al. (2014) Auditory spatial attention representations in the human cerebral cortex. *Cereb Cortex* 24(3):773–784.
28. Saint-Amour D, De Sanctis P, Molholm S, Ritter W, Foxe JJ (2007) Seeing voices: High-density electrical mapping and source-analysis of the multisensory mismatch negativity evoked during the McGurk illusion. *Neuropsychologia* 45(3):587–597.
29. Friedman HR, Goldman-Rakic PS (1994) Coactivation of prefrontal cortex and inferior parietal cortex in working memory tasks revealed by 2DG functional mapping in the rhesus monkey. *J Neurosci* 14(5 Pt 1):2775–2788.
30. Martino J, et al. (2013) Analysis of the subcomponents and cortical terminations of the perisylvian superior longitudinal fasciculus: A fiber dissection and DTI tractography study. *Brain Struct Funct* 218(1):105–121.
31. Hampshire A, Chamberlain SR, Monti MM, Duncan J, Owen AM (2010) The role of the right inferior frontal gyrus: Inhibition and attentional control. *Neuroimage* 50(3): 1313–1319.
32. Maess B, Koelsch S, Gunter TC, Friederici AD (2001) Musical syntax is processed in Broca's area: A MEG study. *Nat Neurosci* 4(5):540–545.
33. Koelsch S (2006) Significance of Broca's area and ventral premotor cortex for music-syntactic processing. *Cortex* 42(4):518–520.
34. Opitz B, Rinne T, Mecklinger A, von Cramon DY, Schröger E (2002) Differential contribution of frontal and temporal cortices to auditory change detection: fMRI and ERP results. *Neuroimage* 15(1):167–174.
35. Musso M, et al. (2003) Broca's area and the language instinct. *Nat Neurosci* 6(7): 774–781.
36. Koelsch S, Gunter TC, Wittfoth M, Sammler D (2005) Interaction between syntax processing in language and in music: An ERP Study. *J Cogn Neurosci* 17(10):1565–1577.
37. Sluming V, et al. (2002) Voxel-based morphometry reveals increased gray matter density in Broca's area in male symphony orchestra musicians. *Neuroimage* 17(3): 1613–1622.
38. Oechslin MS, Imfeld A, Loenneker T, Meyer M, Jäncke L (2009) The plasticity of the superior longitudinal fasciculus as a function of musical expertise: A diffusion tensor imaging study. *Front Hum Neurosci* 3:76.
39. Ojanen V, et al. (2005) Processing of audiovisual speech in Broca's area. *Neuroimage* 25(2):333–338.
40. Sluming V, Brooks J, Howard M, Downes JJ, Roberts N (2007) Broca's area supports enhanced visuospatial cognition in orchestral musicians. *J Neurosci* 27(14):3799–3806.
41. Greicius MD, Supekar K, Menon V, Dougherty RF (2009) Resting-state functional connectivity reflects structural connectivity in the default mode network. *Cereb Cortex* 19(1):72–78.
42. Damoiseaux JS, Greicius MD (2009) Greater than the sum of its parts: A review of studies combining structural connectivity and resting-state functional connectivity. *Brain Struct Funct* 213(6):525–533.
43. Oldfield R (1971) The assessment and analysis of handedness: the Edinburgh inventory. *Neuropsychologia* 9(1):97–113.
44. Ille N, Berg P, Scherg M (2002) Artifact correction of the ongoing EEG using spatial filters based on artifact and brain signal topographies. *J Clin Neurophysiol* 19(2):113–124.
45. Geddes LA, Baker LE (1967) The specific resistance of biological material—a compendium of data for the biomedical engineer and physiologist. *Med Biol Eng* 5(3): 271–293.
46. Cho J-H, Vorwerk J, Wolters CH, Knösche TR (2015) Influence of the head model on EEG and MEG source connectivity analyses. *Neuroimage* 110:60–77.
47. Niso G, et al. (2013) HERMES: Towards an integrated toolbox to characterize functional and effective brain connectivity. *Neuroinformatics* 11(4):405–434.
48. Zalesky A, Fornito A, Bullmore ET (2010) Network-based statistic: Identifying differences in brain networks. *Neuroimage* 53(4):1197–1207.
49. Xia M, Wang J, He Y (2013) BrainNet Viewer: A network visualization tool for human brain connectomics. *PLoS One* 8(7):e68910.
50. Rubinov M, Sporns O (2010) Complex network measures of brain connectivity: Uses and interpretations. *Neuroimage* 52(3):1059–1069.